Journal of Materials Science: Materials in Engineering

ORIGINAL PAPER Open Access

Prediction of 28-day compressive strength of high-slag concrete by establishing accelerated oven curing regimes for rapid quality control

Sudin Mohan[1*], Mohammad Ajmal[2] and Michal P. Drewniok[3]

Abstract

High slag concrete (HSC) offers substantial benefits in terms of durability and reduced carbon footprint, but its late strength gains delayaccurate 28-day strength prediction from early strength. This study aims to develop accelerated oven curing regimes to predict the 28-day compressive strength of HSC accurately. The research focuses on the fundamental question of whether the application of accelerated curing at specific temperatures would help estimate HSC's long-term strength. To achieve this, a series of concrete specimens were subjected to accelerated oven curing at 50 °C and 70 °C. The compressive strength development was observed and correlated with standard curing conditions. Additionally, the hydration kinetics of the cementitious paste under these elevated temperatures were examined by using the isothermal calorimetry method. This research will produce a predictive model correlating accelerated curing data with 28-day strength. The findings of this study will provide a reliable method for estimating the strength of HSC at an early age, enabling more efficient construction planning.

Keywords Calcium silicate hydrate gel, Calcium hydroxide, Alumino ferrite trisulphate, Alumino ferrite monosulphate, Delayed ettringite formation, Tricalcium silicate, Dicalcium silicate

Introduction

There was a time when Portland cement (OPC) was considered the sole binding material in concrete. The Portland cement exhibits higher carbon emissions in traditional concrete. It became a persistent challenge for the construction industry dealing with decarbonisation, and therefore, concrete mixes with cement replacement using supplementary cementitious materials (SCMs) allow for a lower carbon footprint of concrete. SCMs like pulverized fly ash (PFA), ground granulated blast furnace slag (GGBFS), silica fume (SF) were introduced and widely used from the mid-twentieth century in the construction industry for a variety of reasons including cost-effectiveness, enhanced durability properties, and its lower carbon dioxide emissions (British standards. 2011).

GGBFS is a by-product of iron production in blast furnaces and is similar to cement, which has hydraulic properties (Matthes et al. 2018). Compared with OPC, GGBFS has a lower embodied carbon value of 155 kg CO_2e/tonne (Embodied and 2 e of UK cement, additions and cementitious material [Internet], 2025). Concrete with cement as a binder is a fundamental building material used globally in the construction industry; therefore, replacing cement with GGBFS is considered to be one of the strategies to decarbonize cement and concrete. It is possible to reach a higher replacement rate (35–95%) (British standards. 2011; BRE 2005) at the same time

*Correspondence:
Sudin Mohan
sudin.m@hotmail.com
[1] Qatar Beton LLC, Doha, Qatar
[2] Doha Technical Laboratories, Mesaieed, Qatar
[3] School of Civil Engineering, University of Leeds, Leeds, UK

improving the ability to resist aggressive agents from penetrating concrete (Cement_Type_Early_Age_Properties_23_Jun_11. (2011)).

In the precast industry, it is extremely difficult to achieve very early age strength, especially within 24 h from pouring for a high GGBFS concrete mix (Korde et al. 2021). The mold turnover is the main profit factor for the precast concrete industry; therefore, it is mandatory to facilitate an accelerated curing method in order to achieve the desired compressive strength for de-shuttering and lifting the precast elements. The higher the curing temperature, the faster the heat of hydration of the concrete (Winter 2009), which is sufficient to produce a significant increase in the early age strength of slag cement concrete (Zulu et al. 2019).

Compressive strength is one of the most critical mechanical properties that determines the load-carrying capacity and durability of concrete (Jha et al. 2020; Institute and BS 8500–1:2023: concrete. Complementary British Standard to BS EN 206: Method of specifying and guidance for the specifier. 2023). The strength of concrete is assessed based on 28-day results. The reason to consider the 28-day compressive strength as a parameter is based on the maturity of the concrete. The strength development of concrete depends on both time and temperature. The concrete strength is a function of the summation of the product of time and temperature. This is called the maturity of concrete.

Maturity = Σ (time × temperature).

The temperature is taken from an origin lying between − 12 and − 10 °C because hydration of the concrete stops when the temperature of the concrete reaches above − 12 °C. However, − 11 °C is usually taken as a datum line for calculating maturity. The curing temperature of the concrete specimen is 20 ± 2 °C (British Standards (2019)). For instance, a fully matured concrete cured at 18 °C for 28 days will be 19,488 °C h; however, in standard calculations, the maturity of the fully cured concrete is taken as 19,800 °C h. This discrepancy should be attributed to the datum value used for the calculation. Hence, compressive strength at 28 days is considered in the industry as a standard to determine the mechanical property of the concrete (Shetty and Jain 2019). As a rapid quality control procedure, it is crucial for a concrete quality control engineer to predict the desired strength at an early age. According to the maturity model using OPC, cube strength results should achieve 46% of characteristic compressive strength in 3 days and 70% in 7 days (Rhodes, et al. 2008). This assures that the cube will achieve the desired compressive strength in 28 days. Whereas in the case of mixes with a higher percentage of GGBFS, the slower, early strength gain is compared with OPC due to reduced availability of CaO (Cement_Type_Early_Age_Properties_23_Jun_11. (2011)). Nevertheless, slag cements exhibit more strength development at later stages (Austin et al. 1992). The reduced availability of CaO in GGBFS is a key factor for slowing down the hydration process (Korde et al. 2021). By increasing the temperature during the curing time, we can increase the early age strength, so by increasing the GGBFS content and decreasing the embodied carbon, we might achieve satisfactory early age strength. Nevertheless, there are no models predicting long-term strength for concretes with high GGBFS exposed to high temperature curing. Knowing the relationship between early age and 28-day compressive strength for concretes with high OPC replacement with GGBFS cured in high temperatures allows precast concrete producers to optimize their production by minimizing associated embodied carbon.

Even though concrete technology has advanced significantly, there is still a noticeable lack of targeted research on predicting the 28-day compressive strength of high slag cement concrete using early-age strength data from accelerated oven curing regimes. The use of maturity methods, isothermal curing, and other predictive techniques for regular Portland cement systems has been the subject of numerous studies; however, the literature to date has not sufficiently addressed the special hydration kinetics and strength development patterns of high slag blends under elevated temperature conditions. Specifically, for high-volume supplementary cementitious material (SCM) systems like slag, the viability of accurately predicting long-term strength performance in a short period of time, that is, within 55 h of casting, remains a crucial knowledge gap.

By creating and evaluating a predictive methodology specifically designed for high slag concrete using a controlled accelerated oven curing regime, this study seeks to close this gap. This study provides a useful framework for quick quality control by establishing a correlation between early-age compressive strength (measured after oven curing) and the typical 28-day strength. In addition to improving knowledge of the early-age behavior of slag-rich mixes under accelerated oven curing conditions, the methodology helps the precast and ready-mix concrete industries optimize their production schedules. By lowering the waiting time for routine compressive strength testing, the results could improve operational efficiency, guarantee early performance specification compliance, and allow for prompt modifications to production procedures or mix design.

Literature review

Mixes that contain GGBFS, particularly in low ambient temperature conditions, demand an extended period of curing in order to achieve sufficient strength

development (Domone and Iiston 2010). Regourd states that the determined activation energy for slag cements exhibits a higher value compared with the activation energy of their corresponding OPC, specifically 50 and 46 $J.mol^{-1}$, respectively (Moranville-Regourd (n.d.)). Therefore, thermal treatment is advantageous for slag cement as it serves as an efficient source of activation energy for the hydration process of slag; thus, it can be regarded as a latent cementitious material as specified above.

When GGBFS is mixed with OPC, the suspension of slag is activated by the elevated pH of the solution, which is attributed to the presence of calcium hydroxide and alkali ions in the pore solution. Both the clinker and the slag undergo reactions simultaneously, resulting in the formation of calcium silicate hydrate (C–S–H), which contributes to the development of strength. The hydration process of GGBFS generally occurs more slowly compared to Portland cement. Furthermore, during the initial stages of hydration, slag can partially function as an inert filler. This filler effect enhances the nucleation and growth of C–S–H by increasing the effective water-to-cement ratio and providing additional nucleation sites (Black 2016).

Enhancing the basicity of slag results in increased hydration of the slag over a specific time period. However, higher replacement levels result in decreased slag hydration, partly due to the reduced availability of portlandite caused by the lower cement content. For comparison, over 80% of the cement in each system had hydrated after 7 days (Whittaker et al. 2014).

The degree of C_3S hydration increases with the addition of slag after 1 and 3 days; however, over a longer period, it remains comparable to that without slag addition. This phenomenon is thought to result from the crystallization of calcium silicate hydrate (C–S–H) on the slag particles (Fig. 1). Additionally, the reduction in calcium ion concentration in the liquid phase plays a prominent role, especially in the case of very finely ground slag (Whittaker et al. 2014).

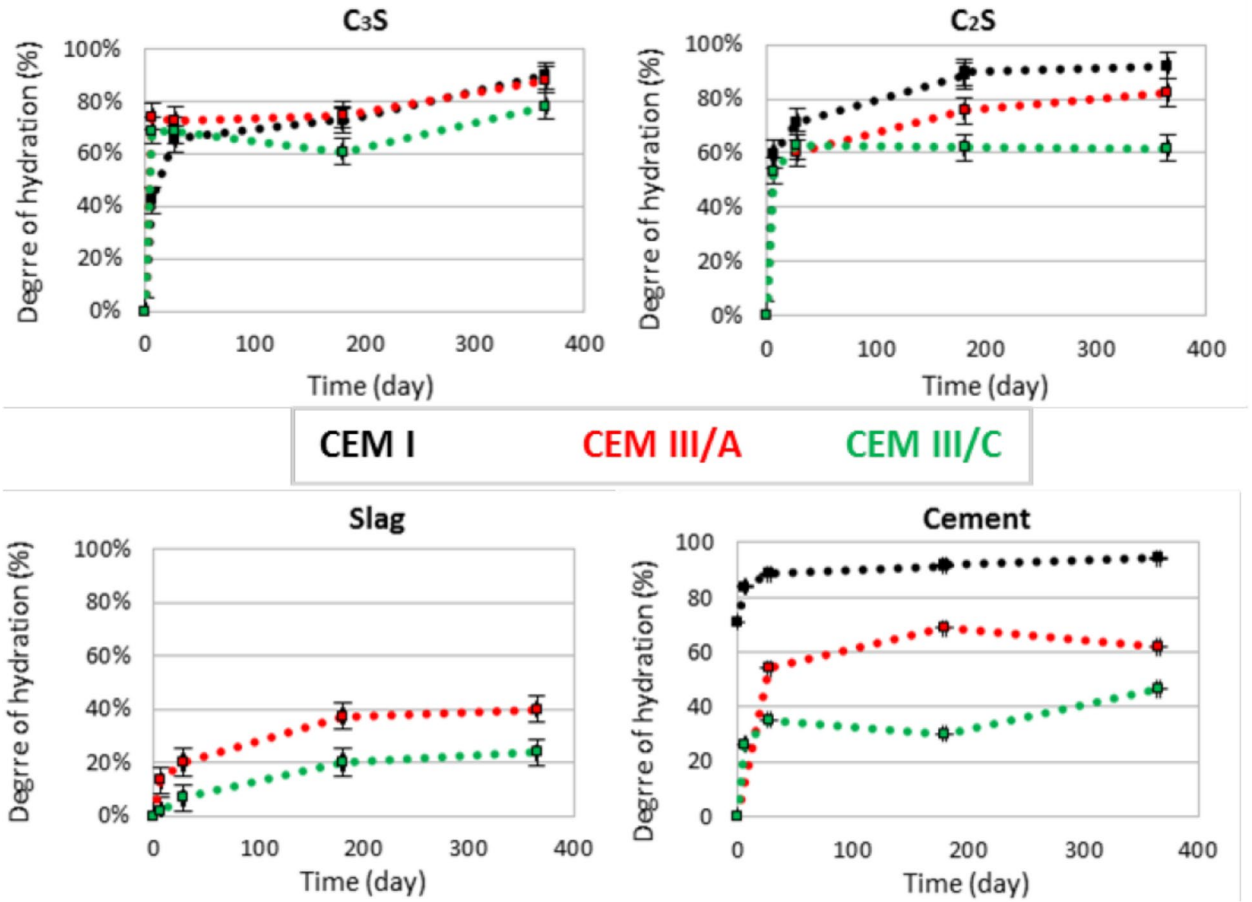

Fig. 1 Example of the graph showing the degree of hydration (%) with respect to time of C_3S, C_2S, slag, and cement for CEM I, CEM III/A, and CEM III/C cement (adapted from Stephant et al. (2015))

The influence of slag on the hydration of C_3A and C_4AF is minimal, as the concentrations of Ca^{2+}, Al^{3+}, and SO_4^{2-} ions in the liquid phase are not significantly altered by the presence of slag. However, because calcium aluminate hydrates and ettringite are well-crystallized and tend to form a porous rather than a compact microstructure, it can be inferred that the hydration rate will be somewhat reduced. Conversely, some calcium hydroxide and SO_4^{2-} ions are adsorbed on the slag glass surface and incorporated into the pozzolanic reaction, which may accelerate the reaction of aluminates (Stephant et al. 2015).

There is a strong correlation between the degree of slag hydration and cement strength. However, as noted by Fierens, varying strengths can be observed at the same hydration degree of different slags, indicating that other factors, such as the microstructure of hydrates and the conditions of their crystallization, also influence strength development (Fierens 1989).

Accelerated curing

Accelerated curing can be conducted in various methods, namely the warm water method, autogenous curing method, and boiling water method (International A (n.d.)). The accelerated curing technique used for this experiment is the oven curing method, which is explained below.

Oven curing method is preferred due to its ease in performing the accelerated test, as no sophisticated setup is needed because every lab will have a thermostatically controlled oven, which is fair enough for conducting an accelerated test by oven curing. Moreover, it is convenient for high slag concrete (HSC) due to its efficiency in providing actual control of curing parameters. This can be achieved by meticulously regulating temperature, a critical factor influencing the hydration of GGBFS. Oven curing facilitates faster strength development without compromising the hardened concrete properties (Wedatalla et al. 2019).

Furthermore, oven curing ensures uniform environmental conditions, minimizing the variations in curing outcomes and enhancing the consistency of strength prediction. This method effectively protects concrete from external influences, ensuring unswerving quality and performance. The accelerated strength gain facilitated by oven curing is advantageous for construction projects demanding pressing timelines (Specifications and for Concrete Structures—2007'Materials and Construction'.2010. 2010).

TNW Akroyd (Akroyd 1961) has conducted an exceptional study on the oven curing method. He performed the oven curing 30 min after mixing the cubes, and it was covered with a base plate once the cubes were placed inside the oven. The temperature was brought to 85 °C within 1 h and maintained at the same temperature for a period of 5 h. After 5 h, the cubes are removed from the oven, stripped, and allowed to cool for 30 min. Then, it is transferred for compressive testing. Akroyd had concluded that the compressive strength test results for cubes cured normally for a period of 7 or 28 days may be predicted by accelerating the curing of the cubes and testing them 29 h after casting (Akroyd 1961).

Effects of accelerated curing on concrete

This section examines the complex mechanisms by which accelerated curing processes influence the fundamental characteristics of concrete. Through a comprehensive analysis of these factors, this study aims to explain the potential advantages and disadvantages of accelerated curing for high-slag concrete, providing valuable insights for optimizing construction practices and achieving desired performance outcomes.

Microstructure

During the accelerated curing process, the elevated temperature and humidity conditions contribute to shortening the induction period of cement hydration (Dorn et al. 2022). There is no change in the main products of hydration like calcium silicate hydrate gel (C–S–H), calcium hydroxide ($Ca(OH)_2$), calcium alumina ferrite (AFt), and monosulphur calcium sulphoaluminate hydrate (AFm) (Kurdowski 2014). Accelerated curing techniques change the morphology, density, atomic ratio, and chain length of C–S–H gels. Under rapid increase in curing temperature changes the bulk density of the ionic structure. The curing temperature affects the atomic distribution and changes the atomic proportions (Wang et al. 2022).

Delayed ettringite formation

Ettringite is a mineral composed of hydrous calcium aluminate sulphate, which undergoes formation within concrete during the process of curing under ambient conditions. However, in situations where concrete is exposed to high-temperature curing, such as in accelerated curing or in the case of mass concrete, the excess heat produced during the process of cement hydration cannot be easily dissipated. As a result, ettringite formation can be delayed. When the concrete is set, it may lead to expansion and result in internal cracking. This phenomenon is called delayed ettringite formation (DEF) (Delayed ettringite formation: in situ concrete. 2001). Nevertheless, prolonged periods of elevated curing result in significantly decreased expansions, which align with documented chemical alterations that may involve the formation of ettringite following heat treatment (Lawrence 1995).

Compressive strength

This parameter requires further elaboration as it is the pivotal property being analyzed in this paper. The compressive strength of concrete refers to the ratio of the maximum uniaxial load that can be sustained by the concrete at a specific rate to the cross-sectional area of a specimen (Perrie 2009). Some of the factors affecting the compressive strength of a concrete specimen are noted below (Neville and Brooks 1994).

Porosity The relationship between water-to-cement ratio and porosity is a significant factor influencing the compressive strength because it affects the porosity of both the cement mortar matrix and the interfacial transition zone between the matrix and the coarse aggregate (Chang 2004).

Water-to-cement ratio Water-to-cement ratio has a direct relation to the strength of concrete due to its natural behavior of awakening of the matrix when increasing the water-to-cement ratio due to an increase in porosity of the mix, whereas it behaves vice versa when the water-to-cement ratio is lowered.

Degree of compaction The strength of concrete is significantly affected by the increased energy applied during compaction. A portion of this strength enhancement may be attributed to unhydrated cement particles being encapsulated by thinner layers of hydrated cement. Additionally, it is plausible that high-pressure-compacted concrete derives its strength from a combination of particulate interlocking, sintering processes, and the hydration of cement (Chang 2004).

Temperature The influence of temperature on concrete strength depends on the time–temperature history of casting and curing, which means the three possibilities: concrete cast and cured at the same temperature, concrete cast at different temperatures but cured at a normal temperature, and concrete cast at normal temperature but cured at different temperatures (Chang 2004).

It has been claimed (Hutchison et al. 1991) that the addition of gypsum to the mix could significantly lessen the adverse effect on strength at later ages after initial high-temperature curing. Normally, gypsum dosage is around 3–5% (Scrivener et al. 2018). This is most likely due to the gypsum interfering with the hydration phases (C_3A and C_4AF) that readily form in the presence of heat. As a result, the later hydration of slower-acting phases (C_2S and C_3S) does not disturb these phases, reducing microstructural damage and enhancing long-term strength.

Many researchers have conducted studies on the 28-day compressive strength of concrete estimation based on early age strength. (Nurse 1949) introduced steam curing, observing inconsistency due to cement composition and hydration rates. Akroyd and Smith-Gander (1956) developed the boiling method, with their modified approach (24-h normal curing + 33-h boiling), which closely aligned with 28-day strengths, eliminating the need for correlation graphs. Ordman and Bondre (1958) highlighted the influence of oven temperature inconsistencies, causing significant under-predictions in high-strength concrete. Neville (1957) demonstrated that smaller cubes tend to over-predict strength, particularly at high compressive levels. Emtroy (1958) presented the Cement and Concrete Association (C.C.A.) curve, providing a standardized and reliable framework for early strength predictions, especially for strengths below 28 MPa. In that, Prof. King's method of accelerated oven curing (Fig. 2) is considered to be more accurate and easier for adoption (Shetty and Jain 2019; Akroyd 1961). For instance, the accelerated oven curing strength of 42 MPa has been increased to more than 65 MPa at 28 days, when it is cured under normal conditions (King 1960 Jun 4). Prof. King cured the cubes at 93 °C for a period of 5 h, and the total time spent for the accelerated curing was 7 h only. Moreover, the aforementioned research was carried out on 100% OPC mix cubes. Whereas over here, we have performed the accelerated oven curing on high slag concrete, and the duration of curing time is more than 24 h.

As previously stated, there exists a range of methods for forecasting the strength of concrete by employing diverse accelerated curing protocols. However, when it comes to concrete with a higher percentage of GGBFS composition, there is a need for further investigation into the effectiveness of accelerated curing using a thermostatically controlled drying oven. The concrete's early strength can be significantly influenced by the increased content of GGBFS. Consequently, it is necessary to thoroughly investigate the correlation between the early strength achieved through accelerated oven curing at various temperatures.

The majority of international standards pertaining to conventional accelerated curing methods have been withdrawn or replaced by other standards, resulting in a lack of a standardized protocol for conducting these tests. Ensuring the precision of forecasts derived from accelerated curing is of utmost importance in order to ascertain the dependability and feasibility of quality control protocols. This can be accomplished by juxtaposing these predictions against the concrete's real-world performance over extended periods of service life.

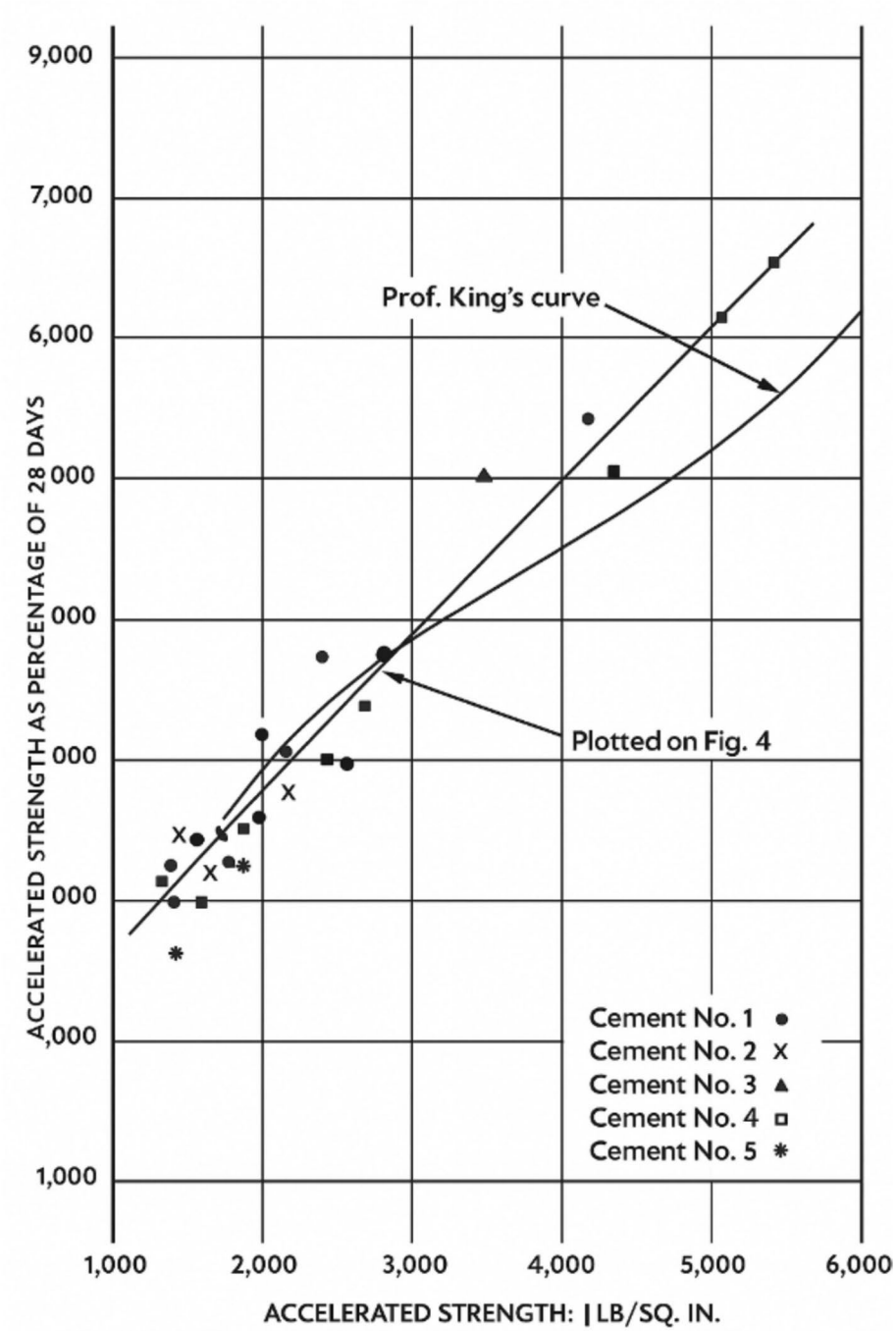

Fig. 2 Prof King's prediction curve for accelerated strength as a percentage of 28 days with respect to the accelerated strength (adapted from Akroyd (1961))

The potential limitations of current predictive models for estimating the 28-day compressive strength in high slag concrete under accelerated curing regimes may pertain to their accuracy and scope. There is a lack of research in the field of developing and validating a reliable predictive model that considers the unique hydration characteristics of slag and its interactions with the accelerated oven curing method. Knowing this relationship allows precast concrete producers

to optimize their production by minimizing associated embodied carbon.

Materials and methods

In this section, we have meticulously analyzed the properties of all constituent materials, i.e., OPC, GGBFS, coarse aggregate and fine aggregate, admixture, and water in order to ensure that constituent materials conform to BS EN 206 (British Standards 2021). The testing of constituent materials was performed based on an international standard (listed in the next sections). The quality control testing and properties of constituent materials are explained below in detail.

Cement

Cements are classified into a number of types based on their application, environment, availability, etc. The most common types of cement used in the Middle East are (i) ordinary Portland cement (OPC) and (ii) sulphate-resistant cement (SRC). For this research, the OPC was adopted due to its availability and consistency in Qatar, where the research took place. The chemical composition of OPC is analyzed in an accredited third-party laboratory, and it complies with BS EN 197–1 (British standards 2011). The OPC (CEM I) used for this study is 42.5 R grade. The chemical composition is given below in Table 1.

The clinker compounds were calculated as per ASTM C 150 (ASTM. ASTM 2021) and displayed in Table 2. Furthermore, C_3A content in this cement is 6.5%, which makes this cement a moderate sulphate-resistant cement even though it is marketed as OPC. The reduction of C_3A content is being pursued in Qatar as a result of the elevated levels of sulphate found in the soil.

Table 2 Clinker compounds of CEM I (OPC)

Clinker compounds	CEM I test results (%)
Alite (C_3S)	65.1
Belite (C_2S)	10.7
Aluminate (C_3A)	6.5
Ferrite (C_4AF)	5.47

There are three main parameters, which are considered by manufacturers for assessing the quality of cement are listed below.

$$\mathrm{LSF}\ (\%) = \mathrm{CaO}/(2.8\mathrm{SiO_2} + 1.2\mathrm{A1_2O_3} + 0.65\mathrm{Fe_2O_3})$$
$$\mathrm{SR}\ (\%) = \mathrm{SiO_2}/(\mathrm{A1_2O_3} + \mathrm{Fe_2O_3})$$
$$\mathrm{AR}\ (\%) = \mathrm{A1_2O_3}/(\mathrm{FE_2O_3})$$

The first one is lime saturation factor (LSF), and it is determined by the ratio of lime to silica, alumina, and iron oxide and governs the relative proportions of C_3S and C_2S. Typical values for LSF are between 92 and % (John and Choo 2003).

The second parameter is silica ratio (SR), which is otherwise called silica modulus. A high silica ratio means that more calcium silicates are present in the clinker and less aluminate and ferrite. Whereas the final parameter alumina ratio (AR) determines the potential relative proportions of aluminate and ferrite phase in the clinker. AR is usually between 1 and 3 (Winter 2009). The

Table 1 Chemical composition of CEM I (OPC) and GGBFS

Chemical components	CEM I test results (%)	BS EN 197–1 limits (%)	GGBFS test results (%)	BS EN 15167–1 limits (%)
Magnesium oxide (MgO)	3.2		4.9	Max.18.0
Aluminium oxide (Al_2O_3)	3.6		13.5	
Silicon dioxide (SiO_2)	20.85		34.21	
Sodium oxide (Na_2O)	0.18		0.16	
Potassium oxide (K_2O)	0.4		0.4	
Calcium oxide (CaO)	63.03		42.90	
Loss of ignition	2.6	Max 5.0	0.9	Max 3.0
Ferric oxide (Fe_2O_3)	1.8		0.9	
Insoluble residue (IR)	0.5	Max 5.0	0.5	Max 1.5
Chlorine (Cl)	0.004	Max.0.1	0.004	Max.0.1
Sulphur trioxide (SO_3)	2.2	Max.3.5	0.5	Max.2.5
CaO/SiO_2 ratio	3.02	Min.2.0		
Titanium oxide (TiO_2)			0.19	

Table 3 Cement parameters

Lime saturation factor (LSF) (%)	93
Silica ratio (SR) (%)	3.86
Alumina ratio (AR) (%)	2

Table 4 GGBFS basicity ratios

Chemical components	Test results (%)	Limits (39) (%)
P1 = CaO/SiO_2	1.25	> 1.0
P2 = $(Cao + MgO)/SiO_2$	1.4	> 1.0
P3 = $(CaO + MgO)/(SiO_2 + Al2O_3)$	1	1.0–1.3
P4 = $(CaO + 0.56Al2O_3 + 1.4\ MgO)/SiO_2$	1.67	> 1.65
P5 = $CaO + MgO + Al2O_3/SiO_2$	1.79	> 1.0

aforementioned parameters for the cement used for this research are tabulated in Table 3.

Winter found that in order to achieve enhanced early strength of cement, it is necessary for the values of SR (silica ratio) and LSF (lime saturation factor) to be elevated (Winter 2009). Nonetheless, there are certain disadvantages associated with the use of high LSF and SR mixes in kilns. These mixes pose significant challenges in terms of achieving the desired reactions, as they are more resistant to combustion and hard to combine. The observed phenomenon is categorized by elevated levels of carbon dioxide (CO_2) emissions, which can be associated with the augmented calcium oxide (CaO) concentration in the cement as well as an enlarged demand for fuel.

Ground granulated blast furnace slag (GGBFS)

The physical and chemical properties of GGBFS used are carefully analyzed by an accredited third-party laboratory. The measured basicity ratios for GGBFS reactivity are tabulated in Table 4.

The significant potential to reduce the mixes' overall carbon footprint is one of the main benefits of using GGBFS as an additional cementitious material in concrete. By decreasing the use of Portland cement (CEM I) and replacing it with one of the most energy and carbon-intensive building materials, i.e., GGBFS, the concrete carbon emission can be reduced significantly. The embodied carbon values calculated (Fig. 3) on a per cubic meter basis for the different mix proportions assessed in this study show the greatest environmental benefit. The total embodied carbon of the concrete significantly decreases when the replacement level of ordinary Portland cement with GGBFS is increased from 50 to 70% (How to calculate the embodied carbon of a concrete mix—factsheet [Internet]. Available from (n.d.)). The strategic application of GGBFS thus supports the development of low-carbon concrete technologies without sacrificing performance requirements and is in line with international efforts to decarbonize the construction industry (Kelly 2023 Jul 3).

Mix proportions

A single grade of mix with three different cementitious combinations is considered for this study. The primary

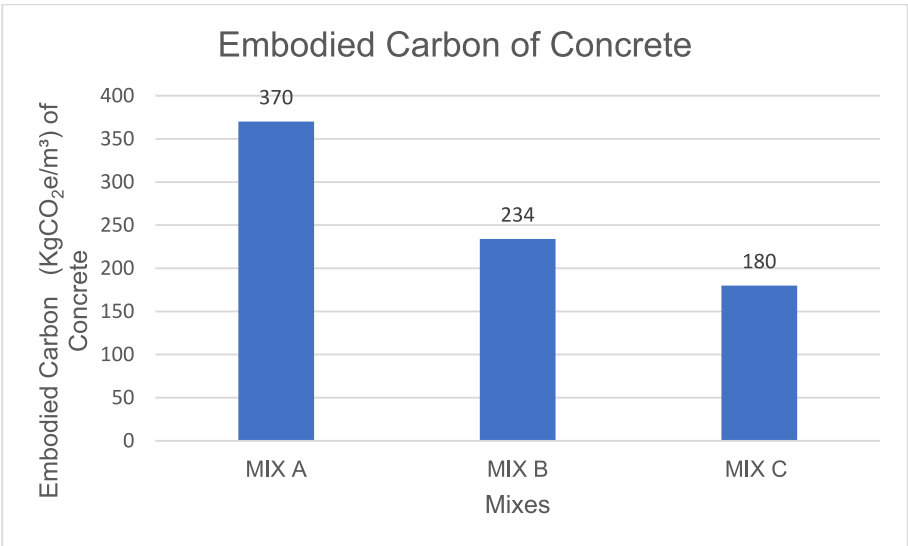

Fig. 3 Embodied carbon of concrete mixes

Table 5 Mix designs

Mix Grade	Mix name	OPC (kg/m^3)	GGBFS (kg/m^3)	Water (kg/m^3)	10/20 mm (kg/m^3)	4/10 mm (kg/m^3)	0/4 mm (kg/m^3)	HP 540 A (kg/m^3)	Air (%)	W/C ratio	Theoretical density (kg/m^3)
C50 OPC	Mix A	410	-	144	778	382	800	4 ± 1.5	2	0.35	2510
C50-OPC + 50%GGBFS	Mix B	210	210	147	771	385	771	4 ± 1.5	2	0.35	2490
C50-OPC + 70%GGBFS	Mix C	129	301	151	759	380	759	4 ± 1.5	2	0.35	2480

objective of adding different GGBFS proportions was to comprehensively investigate the influence of a wide range of GGBFS additions on concrete properties. All the mixes are designed to be C50 grade. The different cementitious combination of the mixes used for this study is given below.

I. C50-OPC 100%
II. C50-OPC + 50%GGBFS
III. C50-OPC + 70% GGBFS

The mix designs are designed in SSD (saturated surface dry) conditions for each cementitious combination. Mix designs are displayed in Table 5 with the yield calculations to ensure that concrete is designed for 1 m^3. Herein, air content in the mix is calculated according to ACI 211.1 (Dixon et al. 1991), which is 2% when the maximum aggregate size is 20 mm. The yield of the mix may be slightly kept higher. However, in reality, the air content would be less than the designed value; hence, the yield would be around 1.02 m^3.

The quantity of admixture in the latter mixes is subject to a tolerance of ± 1.5 kg/m^3 due to ambient conditions and the presence of moisture in the fine aggregate.

Mixing procedure

A total of 45 cube moulds per trial mix of size 150 mm × 150 mm × 150 mm are arranged to make cube specimens. Upon the completion of the entire trial, i.e., 9 trials, a total of 405 concrete cubes were cast. It was observed that the concrete had achieved final setting within a period of 17–20 h after casting. Consequently, the demoulding of the cubes was carried out within this specific timeframe. The cubes were stored within the laboratory for a duration of 22 h subsequent to their casting, after which they were deemed suitable for transportation to a third-party laboratory for the purpose of conducting tests. During the transportation process, gunny bags were utilized to cover the concrete cubes in order to mitigate moisture loss. The cube specimens were made in accordance with the BS EN 12390–2 (11). Figure 4 depicts the activity versus time graph to understand the timeline of sampling until testing.

The 27 cubes were subjected to the standard water curing regime specified by BS EN 12390–2 (British Standards 2019). The temperature of the water used for curing in the tank was adjusted to 20 °C. Within the set of 27 cubes, there are 9 cubes designated for each of the three age groups: 7 days, 14 days, and 28 days, respectively. These cubes are specifically allocated for the purpose of conducting compressive strength tests in accordance with BS EN 12390–3 (British Standards 2019). The schematic flow of the complete trial mix procedure is depicted below.

Isothermal calorimetry

The isothermal calorimetry test was conducted to study the hydration of cementitious. The relationship between accelerated oven-cured strength and concrete subjected to water curing at different ages has been well studied in this project. A calorimetry test was performed on accelerated oven-cured mixes to monitor the hydration kinetics. The isothermal calorimeter has to be placed in an environment with a constant temperature, typically a high-precision thermostat, in order to accurately measure heat. It is crucial to verify the accuracy of the thermostat's temperature setting. The calorimetry tests have several applications, the determination of heat of hydration, estimating the activation energy, cement admixture interactions, etc. ().

Accelerated oven curing procedure

The remaining 18 cubes were subjected to oven curing in two distinct thermostatically controlled electric drying ovens, with each oven accommodating 9 cubes. The drying oven was calibrated and can conduct a heat up to a range from 20 to 250 °C.

The Canadian precast/prestressed concrete Institute endorses a curing temperature range of 60 to 70 oC for high-performance precast concrete (TECHNICAL GUIDE. (n.d.)). Although there is a relatively small difference in the effectiveness of curing within this range, an optimum curing temperature of 50 °C has been selected, with a maximum permissible temperature of 70 °C.

The ovens were set to different target temperatures, 50 °C and 70 °C, and the oven curing was restricted to 24 ± 0.5 h. In the experiment involving specimens with a target curing temperature of 50 °C, the cubes were initially cured at a temperature of 30 °C for a duration of 2 h. Subsequently, the curing temperature was raised to 50 °C for the remaining duration of the oven curing process. Whereas, in the case of a 70 °C oven curing setup, the specimens were initially cured at a temperature of 30°C for a duration of 2 h. Subsequently, the temperature was raised to 50°C and maintained for 1 h. Finally, the specimens were subjected to the desired curing temperature of 70°C for the remaining curing period, which lasted for 24 ± 0.5 h. The temperature time flow for 50°C was depicted below in Fig. 5. The time–temperature relation was similar to the 70°C Curing regime except temperature progression style as stated in previously.

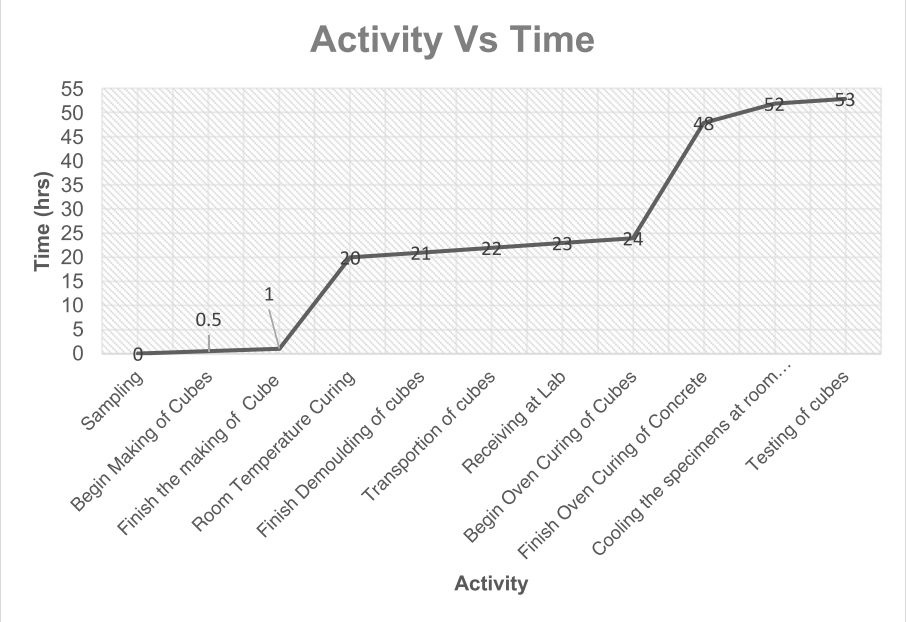

Fig. 4 Schematic flow of trial mix from beginning to end

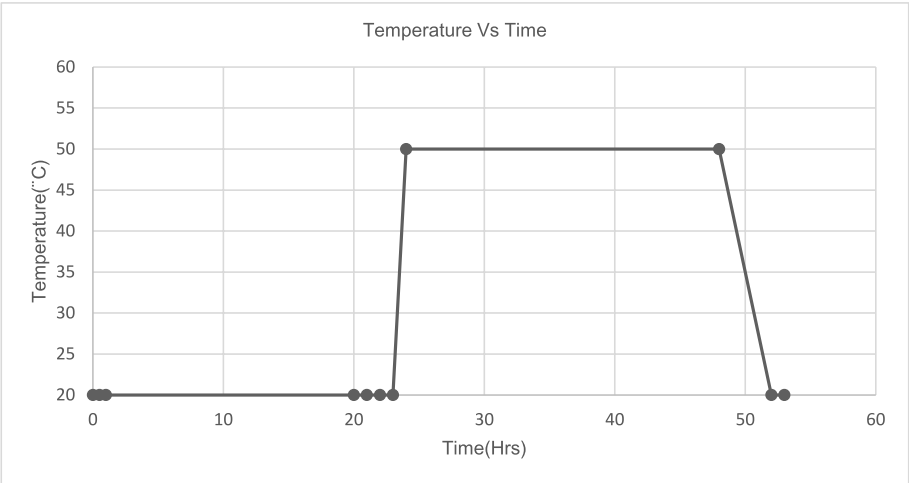

Fig. 5 Time–temperature flow of experiment for 50 °C

Following the removal of the cubes from the oven, a designated cooling period of approximately 4 to 5 h was observed, and the cubes were subjected to compressive testing of concrete as per BS EN 12390–3 (British Standards 2019). The results of compressive strength of cubes are reported separately for cubes cured at different accelerated oven curing regimes, that is, 50 °C and 70 °C.

Results

The three mixes with fourth-generation high-range PC admixture with a solid content of more than 35% are used for high workability for pumping. Initially, elevated pumping pressures are necessary to overcome the frictional resistance between the concrete and the pump tube. Once this initial resistance is mitigated and a smooth interface is established, the required pumping pressure can be reduced. A sustained decrease in pumping pressure relative to the initial value signifies satisfactory flowability characteristics of the high-performance

concrete (HPC) mix containing the slag. Hence, the target slump of 200 ± 40 mm for better workability due to high GGBFS replacement, and the maximum target temperature is 35 °C (Institute and ACI 305.1 Specification for hot weather concreting [Internet]. 2014). The higher slump was proposed the cube specimens were made in accordance with the BS EN 12390–2 (British Standards 2019). It was observed that the concrete had achieved final setting within a period of 17–20 h after casting. Subsequently, the aforementioned curing regimes of the specimens, conduction calorimetry, and compressive strength test were conducted. The results have been elaborated below.

Conduction calorimetry

The heat flow of the OPC + GGBFS mixes is presented below. For 50 °C, the highest first peak was for OPC, lower for 50% GGBFS, and the lowest for 70% GGBFS cement replacement. It was noticeable that for the highest cement replacement, the first peak was delayed. For 50% OPC replacement, delay was not noticed (Fig. 6).

For 70 °C, the highest first peak was for OPC, lower for 50% GGBFS, and the lowest 70% for GGBFS cement replacement. For both 50% and 70% OPC replacement with GGBFS, the first peak was slightly delayed compared with 100% OPC (Fig. 7).

Morphology by scanning electron microscopy (SEM)

The morphology of cement paste was examined using scanning electron microscopy (SEM) in back-scattered electron (BSE) imaging mode. The cement combinations for all three mixes were cured at two different temperatures: 50°C and 70°C. The curing lasted for 24 h in a sealed environment to prevent drying out, which is typical in accelerated oven curing. After curing, hydration stoppage is performed as recommended in

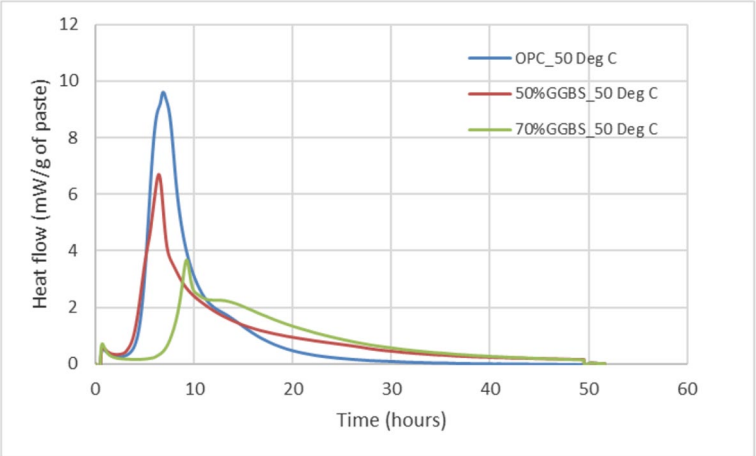

Fig. 6 Calorimetry graph at50 °C

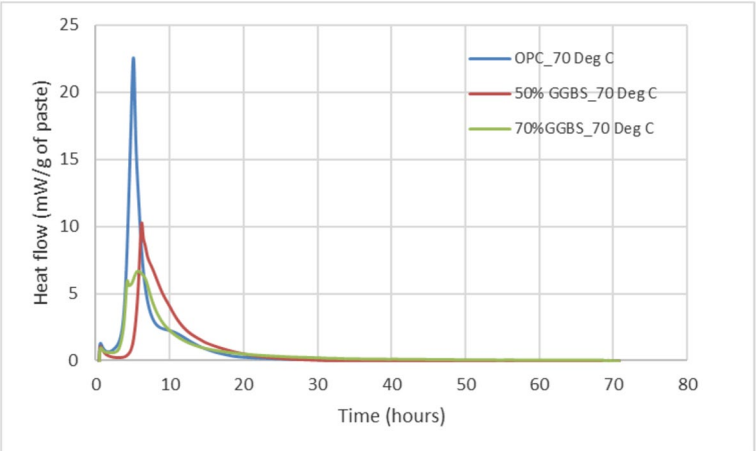

Fig. 7 Calorimetry graph at70 °C

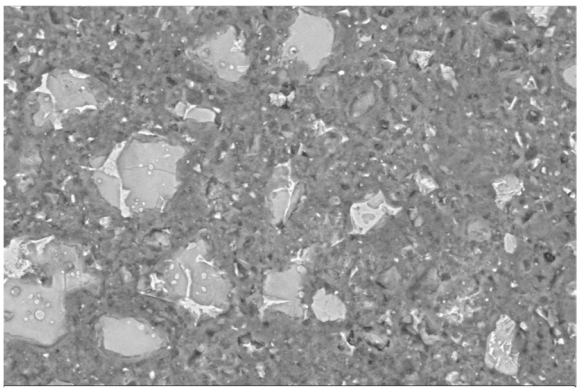

Fig. 8 SEM image of C50 OPC mix at 50 °C

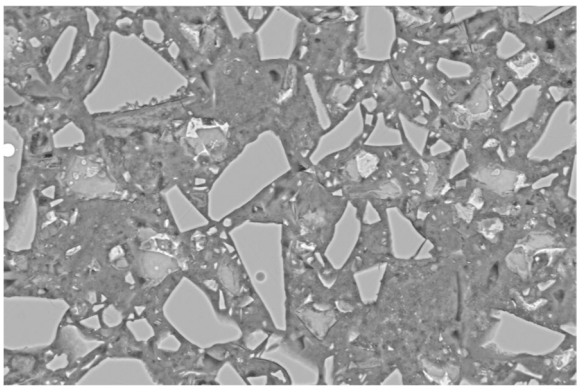

Fig. 9 SEM image of C50 OPC + 50% GGBFS mix at 50 °C

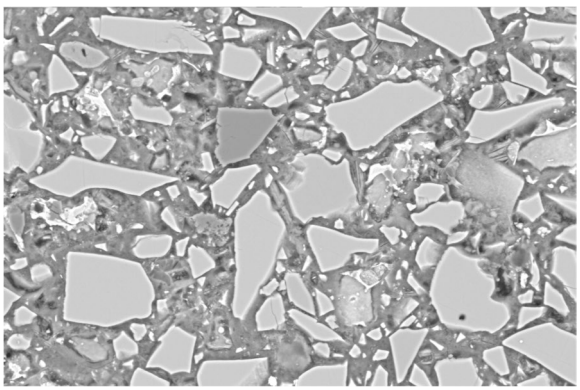

Fig. 10 SEM image of C50 OPC + 70% GGBFS mix at 50 °C

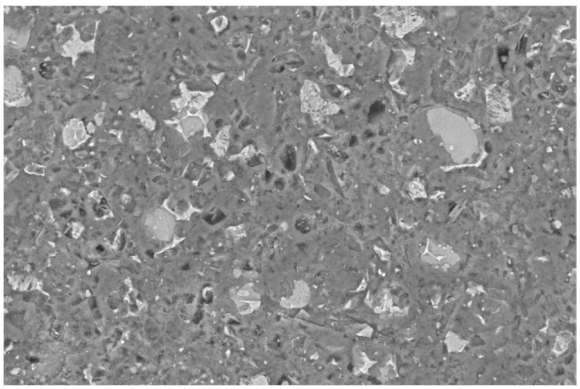

Fig. 11 SEM image of C50 OPC + 70% GGBFS mix at 50 °C

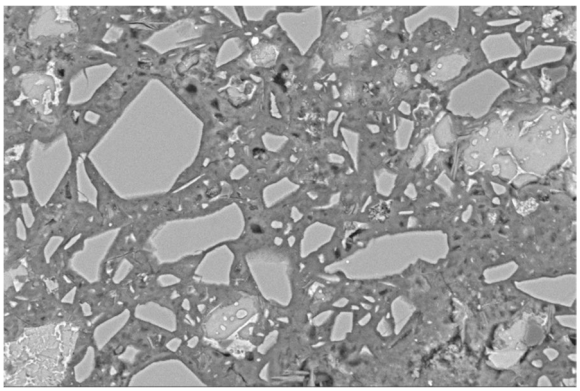

Fig. 12 SEM image of C50 OPC + 50% GGBFS mix at 70 °C

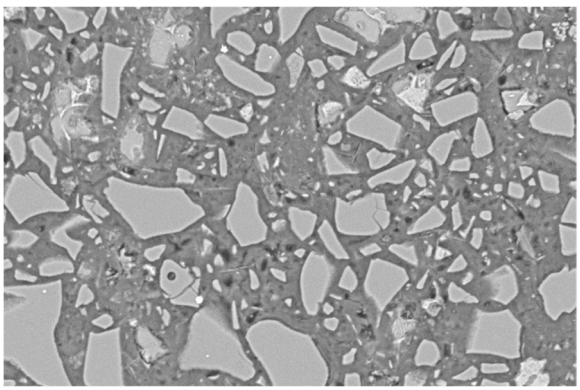

Fig. 13 SEM image of C50 OPC + 70% GGBFS mix at 70 °C

RILEM TC-238 (Snellings et al. 2018 Dec 13) by solvent exchange, then the samples were impregnated with epoxy resin, subsequently polished and coated with a conductive carbon layer, and analyzed in the SEM. The images of all the oven-cured cement combinations are shown below. The main goal of this analysis was to determine if high-temperature curing causes noticeable changes at the microstructural level (Figs. 8, 9,10, 11, 12, and 13).

In the C50 full OPC mix, it is clear that the cement particles are mostly rounded with sizes between 10 and 20 µm, which is the usual range for cement grain size. There

are some polished areas with visible relief, especially in high-slag mixes. This is likely due to the more brittle nature of slag-rich hydration products. This phenomenon is common and does not affect the interpretation of the microstructure. Porosity seems to increase when the curing temperature rises from 50 to 70°C (Xu et al. 2023 Oct). Irregular shapes seen on the otherwise rounded CEM I particles in Fig. 9 may be due to minor impurities in the cement.

In contrast, mixes that include slag show a decrease in porosity compared to pure CEM I mixes. This demonstrates the positive effect of using supplementary cementitious materials (SCMs) like fly ash and GGBFS to lessen the negative impacts of heat curing. This likely results from ongoing pozzolanic reactions that help densify the matrix, even at higher temperatures.

In the C50 OPC + 50% GGBFS mix, which has more slag than the C50 OPC + 30% GGBFS mix, Fig. 11 shows a denser matrix with angular slag particles clearly visible above the cement particles. The average size of GGBFS particles is smaller than 10 µm (Divsholi et al. 2014 Jun 20). These angular shapes are also less resistant to polishing, which can create minor surface artifacts.

Microcracks are faintly visible in pastes cured at 70°C, likely due to drying out from the evaporation of physically bound water in C–S–H pores. AFm phases appear as small plate-like crystals embedded in the dense C–S–H matrix in all BSE images. These are among the hydration products that contribute to overall matrix densification. While these plate-like structures may look needle-like in cross-section, they should not be confused with ettringite, which is truly acicular-shaped. AFm phases are better classified as platelets (Taylor and Cement chemistry. T. Telford 1998; Winter 2012).

In the C50 OPC + 70% GGBFS mix cured at 70°C, the microstructure shows fewer visible crystalline phases, likely due to the high reactivity of slag at elevated temperatures. The microstructure appears to have a higher proportion of amorphous C–S–H and fewer distinct CH crystals, indicating strong pozzolanic activity and significant use of portlandite." As expected in high-slag mixes, the amount of calcium hydroxide (CH) is low.

This study did not perform elemental mapping using energy ispersive X-ray spectroscopy (EDX). SEM along with EDX would provide a more thorough microstructural characterization, particularly in identifying the spatial distribution of clinker phases, slag, and hydration products.

Compressive strength results

The main aim of this study was to find the relation between accelerated oven-cured specimens and water-cured specimens for establishing a prediction model. In order to establish a prediction model, monitoring of the compressive strength of specimens was inexorable.

Cube specimens have undergone the accelerated oven curing regimes, and cubes cured under the water curing regime as per BS EN 12390–2 (British Standards (2019)). The cubes cured under water curing have been tested for different ages, that is, 7 days,14 days, and 28 days.

A comparison has been made between the compressive strength of average accelerated oven-cured 4 specimens at 23 h from casting and 28-day water-cured specimens (see Figs. 14 and 15). This was done by creating two bar graphs to analyze the trend of strength gain for each mix at two different curing temperatures. The two bar

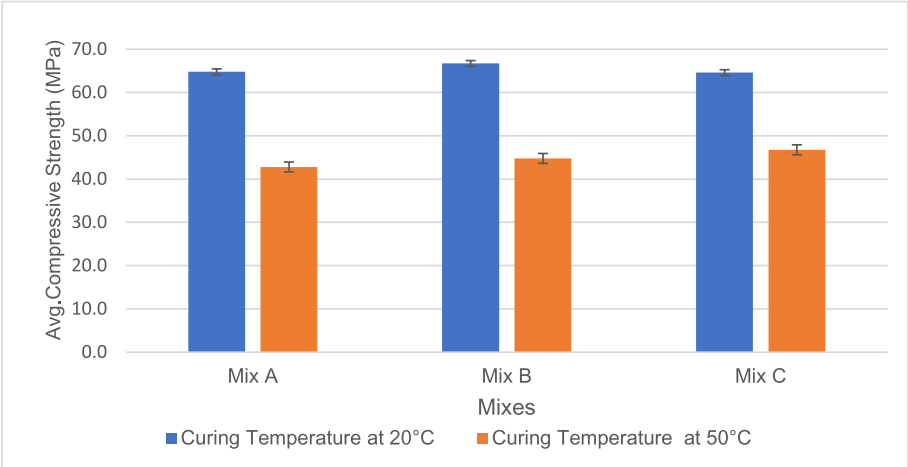

Fig. 14 Comparison between 28 days compressive strength versus accelerated oven cured strength at 50 °C (mix A—C50 OPC, mix B—C50-OPC + 50%GGBFS, and mix C—C50-OPC + 70%GGBFS)

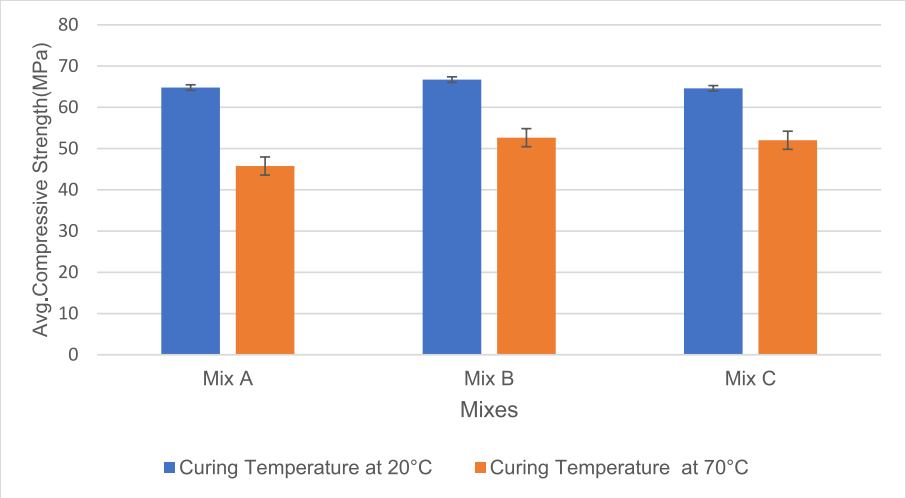

Fig. 15 Comparison between 28-day compressive strength versus accelerated oven cured strength at 70 °C (mix A—C50 OPC, mix B—C50-OPC + 50%GGBFS, and mix C—C50-OPC + 70%GGBFS)

graphs are depicted below. All mixes, regardless of OPC replacement, achieved 68 ± 8 MPa after 28 days of curing in ambient temperature (see Figs. 14 and 15). Concretes with OPC replacement with GGBFS had slightly higher compressive strength compared with OPC when cured at 50 °C (Fig. 14). The same trend follows for accelerated curing at 70 °C; however, there was not much difference in the compressive strength between 50 and 70% cement replacement. The difference between the percentage strength gain attained by accelerated curing regimes and curing in standard conditions was higher for samples subjected to accelerated curing at 50 °C and smaller for samples subjected to accelerated curing at 70 °C and was noticed as shown in Table 6.

Discussion

The discussion of our results has been divided into two main sections. In the first part, we emphasize the hydration kinetics in different curing regimes based on the isothermal calorimetry, whereas the second part focuses on the prediction of actual compressive strength from accelerated cured concrete strength results.

a . The isothermal calorimetry was conducted on all mixes at two distinct temperatures, namely 50° and 70°. It was noticed that the heat flow rate is higher in the full OPC mix, and as the slag content of the mix is getting higher, the heat flow also decreases. It is clearly depicted in Figs. 3 and 4. That is the main reason for mass concrete in order to reduce the core temperature of the structural element, with the higher cement replacement with SCMs being recommended. The GGBFS hydrates at a slower rate than OPC, which produces a lower temperature rise (CIRIA (2007).

b After the initial reaction, there is an induction period, which is otherwise called the dormant period. The gypsum in cement is used to prevent flash set. It is usually added 3–5% with respect to seasonal changes, and retarders are used to prolong the setting time. Hence, the induction period of GGBFS mixes is higher than that of OPC mixes. The induction period would also be higher in mixes containing retarders. Acceleratory period where you can notice a spike indicating C_3S and C_2S hydration. Here comes the deceleratory period where hydration slows down; in our case, it is happening after 10 h in the GGBFS mix

Table 6 Strength gain analysis

Mixes	% of average strength gain in 28 days from50°C cured specimen	% of average strength gain in 28 days from70°C cured specimen
C50-OPC	33.9	29.5
C50-OPC + 50%GGBFS	32.7	21.1
C50-OPC + 70% GGBFS	27.5	19.5

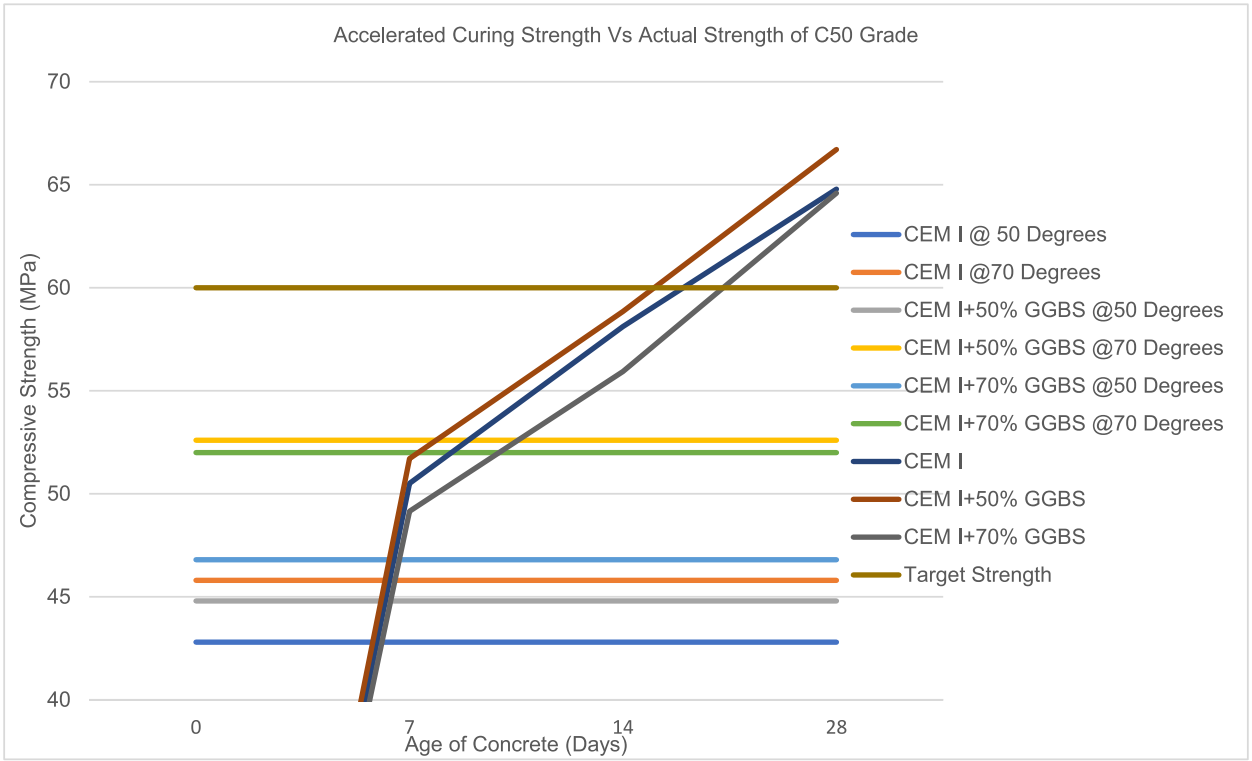

Fig. 16 Compressive strength prediction graph

at 50°. However, at elevated temperatures, the hydration slows down for around 6 h for GGBFS mixes. In the case of OPC mixes, deceleration is almost similar, even though in high temperatures, sudden deceleration is observed. The deceleration period in cement hydration is a complex process influenced by mineral composition, temperature, and its water-to-cement ratio. C_3S hydrates rapidly initially, leading to acceleration, but it slows down as water decreases and products accumulate. C_2S hydrates more slowly and contributes to later-age strength. Elevated temperature accelerates initial C_3S hydration but can also decrease product solubility, leading to pronounced deceleration. Lower temperatures slow down both acceleration and deceleration. GGBFS can delay initial hydration and accelerate C_2S hydration at elevated temperatures. OPC, primarily C_3S and C_2S, experiences rapid initial hydration followed by deceleration. Elevated temperatures can cause sudden deceleration due to increased product solubility (Qi et al. 2021 Feb 1)

In the next phase, gypsum started to deplete and forms monosulphate. The Ettringite (Aft) is the one which converts to monosulphate (Linderoth et al. 2021). This phase is called sulphate depletion phase.

c The prediction graph is constructed using the compressive strength test data mentioned earlier in order to estimate the 28-day compressive strength of mixes A, B, and C. This estimation is based on the compressive strength results obtained from accelerated oven-cured samples that were subjected to two different curing temperatures. The developed prediction model is established as the main goal of this study, and it is noticed that an average strength difference between accelerated oven-cured specimens cured at 70° and cubes° tested at 28 days is around 21% for mix B, whereas for mix C, it is 19.53%. This number is quite high in mix A, which is 35%.

The prediction graph is established and displayed below and can be used for predicting the 28-day compressive strength of concrete from accelerated oven-cured compressive strength results. In the prediction graph, the target strength is calculated as 59.8 MPa (Guide to evaluation of strength test results of concrete 2011). The average strength gain in 28 days is analyzed from accelerated oven-cured specimens compressive strength is tabulated in Table 6. The trend of this strength is clearly visible in Fig. 16.

Limitation of the analysis

The scope of this study was limited to a single grade with two different compositions of GGBFS under two distinct temperatures only. In order to validate the developed model, future research should investigate the accelerated oven curing at 70 °C for all grades of concrete with GGBFS compositions ranging from 35 to 70%.

Conclusion

This study is set out to predict the 28-day compressive strength of high slag concrete by establishing the accelerated curing regimes. The findings of this investigation are delineated in the subsequent sections.

- For analyzed temperatures and levels of OPC replacement with GGBFS, the prediction graph shows the evident correlation between the accelerated oven-cured compressive strength and the 28-day compressive strength. By examining the accelerated strength achieved at two distinct temperatures, it is possible to anticipate the compressive strength of concrete at 28 days.
- This study has identified that a curing temperature of 70 °C is closer to the 28-day compressive strength. In other words, the percentage of average strength gained in 28 days from 70 °C cured specimens across all mix types amounts to merely 23.33%, whereas the average strength gained in 28 days from 50°C cured specimens is 31.42%.
- The mix of OPC + 70%GGBFS tends to achieve greater strength gain in 70 °C curing temperature, and average strength gained in 28 days from 70°C is comparatively lower that is 19.53%. Hence, oven curing temperature of 70 °C can be considered as regarded as the closest accelerated curing temperature for high slag concrete.
- This study observes that the induction period for mix C is higher than that of other mixes. However, in the acceleratory period, higher heat release is observed on mix A, which is 9.8 mW/g for specimens cured at 50 °C and 23.2 mW/g for specimens cured at 70 °C.

Future research should look into a broader range of curing profiles beyond the constant 70 °C condition. This includes changes in temperature, duration, and possible use of stepped or cyclic curing methods. These studies could help find the most effective and practical curing methods for specific engineering needs and concrete performance goals.

Moreover, more studies are necessary to assess the impact of accelerated oven curing with different levels of ground granulated blast furnace slag (GGBFS) replacement, especially between 35 and 95%. This will help identify the best mix that balances early strength with long-term durability under accelerated curing conditions.

A thorough microstructural analysis of the concrete exposed to elevated-temperature curing is also crucial. Techniques like scanning electron microscopy (SEM) with EDX for elemental mapping, X-ray diffraction (XRD), and the nitrogen adsorption method should be used to evaluate how high-temperature curing affects hydration products, porosity, and the stability of the cement matrix.

Finally, testing specific to performance, such as shrinkage, creep, sulfate resistance, and chloride permeability, should be conducted to understand how the accelerated curing method affects durability and long-term service life of concrete, particularly in high-performance or precast concrete applications.

Acknowledgements

The authors wish to acknowledge with gratitude Mr. Imran Khan Bhati from Qatar Beton Readymix for providing an ample quantity of concrete for the research.

Author contributions

Author A: Conceptualization, Methodology, Data Curation, Formal Analysis.
Author B: Literature Review, Writing – Original Draft, Validation.
Author C: Supervision, Writing – Review & Editing.

Data availability

The data collected and analyzed in this study are available from the corresponding author on reasonable request.

Declarations

Competing interests

The authors declare that they have no competing interests.

Received: 31 January 2025 Accepted: 18 August 2025
Published online: 30 September 2025

References

Akroyd TNW (1961) The accelerated curing of concrete test cubes. Proc Inst Civ Eng 19(1):1–22
Akroyd TNW, Smith-Gander SE (1956) The prediction of the 28-day strength of concrete from its early strength. Mag Concr Res 8(23):83–88
American Concrete Institute (2011) Guide to evaluation of strength test results of concrete. ACI 214R-11. Farmington hills, MI: American Concrete Institute.
American Concrete Institute (2014) ACI 305.1 Specification for hot weather concreting. Available from: http://concrete.org/Publications/
ASTM (2021) ASTM C 150/C150M - 21 : specification for Portland cement. Vol. ASTM C 150/C150M-21. West Conshohocken, PA: ASTM International. Available from: http://www.astm.org/cgi-bin/resolver.cgi?C150C150M-21
Austin SA, Robins PJ, Issaad A (1992) Influence of curing methods on the strength and permeability of GGBFS concrete in a simulated arid climate. Cem Concr Compos. https://doi.org/10.1016/0958-9465(92)90009-K
Black L (2016) Low clinker cement as a sustainable construction material. In: Sustainability of construction materials. Woodhead Publishing, London Elsevier; 415–57
BRE (2005) Concrete in aggressive ground. Special Digest 1

British Standards Institution (2011) BS EN 197-1:2011. Cement – Part 1: Composition, specifications and conformity criteria for common cements. London: British Standards Institution. Available at: https://knowledge.bsigroup.com/products/cement-composition-specifications-and-conformity-criteria-for-common-cements
British Standards Institution (2019) BS EN 12390-2:2019. Testing hardened concrete – Part 2: Making and curing specimens for strength tests. London: British Standards Institution. Available at: https://shop.bsigroup.com/products/testing-hardened-concretemaking-andcuring-specimens-for-strength-tests
British Standards Institution (2019) BS EN 12390-3:2019. Testing hardened concrete – Part 3: Compressive strength of test specimens. London: British Standards Institution. Available at: https://shop.bsigroup.com/products/testing-hardened-concretecompressive-strength-of-test-specimens. Accessed 3 Sept 2025
British Standards Institution (2021) BS EN 206:2013+A2:2021. Concrete – Specification, performance, production and conformity. London: British Standards Institution. Available at: https://shop.bsigroup.com/products/concrete-specification-performanceproduction-and-conformity
British Standards Institute. BS 8500–1:2023: concrete. Complementary British Standard to BS EN 206: method of specifying and guidance for the specifier. 2023.
CIRIA (2007) C660: Early-age thermal crack control in concrete. London: CIRIA. Available at: https://www.ciria.org/Resources/Free_publications/C660
Concrete Centre (2011) Cement type early-age properties. [Technical report]. London: Concrete Centre
Chang PK (2004) An approach to optimizing mix design for properties of high-performance concrete. Cem Concr Res 34(4):623–629
Delayed ettringite formation: in situ concrete. (2001) Vol. BRE IP11/01. British Research Establishment
Dixon DE, Prestrera JR, George U Burg SR, Abdun-Nur EA, Barton Leonard W Bell SG, Blas SJ, et al. (1991) Standard practice for selecting proportions for normal, heavyweight, and mass concrete (ACI 211.1–91) Chairman, Subcommittee A
Divsholi BS, Lim TYD, Teng S (2014) Durability properties and microstructure of ground granulated blast furnace slag cement concrete. Int J Concr Struct Mater 8(2):157–164
Domone P, liston J (2010) Construction materials: their nature and behavior. Spon Press, Oxon
Dorn T, Blask O, Stephan D (2022) Acceleration of cement hydration—a review of the working mechanisms, effects on setting time, and compressive strength development of accelerating admixtures. Constr Build Mater 323:126554
Embodied CO 2 e of UK cement, additions and cementitious material (2025) Available from: chrome extension://efaidnbmnnnibpcajpcglclefindmkaj/https://cement.mineralproducts.org/MPACement/media/Cement/Publications/Fact-Sheets/FS_18_Embodied_CO2e.pdf. Cited 2025 Aug 4.
Emtroy (1958) The estimation of the strength of concrete from its early strength. Cementand Concrete Association
Fierens P (1989) The hydration and properties of slags. CANMET Special Publication; CANMET, Ottawa, Canada, 35–45
How to calculate the embodied carbon of a concrete mix—factsheet (n.d.) Available from: https://www.alcas.asn.au/auslci-emissions-factors
Hutchison RG, Chang JT, Jennings HM, Brodwin ME (1991) Thermal acceleration of Portland cement mortars with microwave energy. Cem Concr Res 21(5):795–799
International A (n.d.) Standard test method for making, accelerated curing, and testing concrete compression test specimens. Available from: www.astm.org
Jha AK, Adhikari S, Thapa S, Kumar A, Kumar A, Mishra S (2020) Evaluation of factors affecting compressive strength of concrete using machine learning. In: 2020 Advanced Computing and Communication Technologies for High Performance Applications (ACCTHPA). IEEE 70–4
Kelly F (2023) A review of GGBS use in the UK and its role in reducing embodied carbon. Struct Eng 101(07):24–27
King JWH (1960) An accelerated test for the seven- and twenty-eight-day compressive strengths of concrete. J Appl Chem 10(6):256–262
Korde C, Cruickshank M, West RP (2021) Activation of slag: a comparative study of cement, lime, calcium sulfate, GGBS fineness and temperature. Mag Concr Res 73(1):15–31
Kurdowski W (2014) Cement and concrete chemistry. Springer, Netherlands, Dordrecht
Lawrence CD (1995) Mortar expansions due to delayed ettringite formation. Effects of curing period and temperature. Cem Concr Res 25(4):903–914
Linderoth O, Wadsö L, Jansen D (2021) Long-term cement hydration studies with isothermal calorimetry. Cem Concr Res 141:106344
Matthes W, Vollpracht A, Villagrán Y, Kamali-Bernard S, Hooton D, Gruyaert E, et al. (2018) Ground granulated blast-furnace slag. 1–53
Moranville-Regourd M (n.d.) Cements made from blastfurnace slag. In: Lea's chemistry of cement and concrete. Butterworth-Heinemann; Oxford, pp 637–678
Neville AM (1957) The influence of the size of the test cube on the strength of concrete. Rilem Bulletin, 2(7), pp 31–38
Neville AM, Brooks JJ (1994) Concrete technology. Harlow Longman Publications. Harlow
Newman J, Choo BS (2003) Advanced concrete technology: constituent materials. Butterworth-Heinemann, Oxford
Nurse, RW (1949) The effect of the cement composition on the strength of concrete. Proceedings of the symposium on the chemistry of cements, London, pp 111–125
Ordman MN, Bondre A (1958) The effect of oven temperature on the strength of high-strength concrete. Rilem Bulletin 2(10):34–40
Perrie B (2009) Strength of hardened concrete. In: Fulton's concrete technology. 9th Edition. Midrand: Cement and Concrete Institute 97–110
Qi T, Zhou W, Liu X, Wang Q, Zhang S (2021) Predictive hydration model of Portland cement and its main minerals based on dissolution theory and water diffusion theory. Materials 14(3):1–34
Rhodes JA, Carreira++ DJ, Beaudoin JJ, Brauson DE, Gamble BR, Geymayer HG, et al. (2008) Prediction of creep, shrinkage, and temperature effects in concrete structures
Scrivener K, Snellings R, Lothenbach B, editors (2018) A practical guide to microstructural analysis of cementitious materials. CRC Press. Boca Raton
Shetty MS, Jain AK (2019) Concrete technology (theory and practice). S. Chand Publishing, New Delhi
Snellings R, Chwast J, Cizer Ö, De Belie N, Dhandapani Y, Durdzinski P et al (2018) Rilem TC-238 SCM recommendation on hydration stoppage by solvent exchange for the study of hydrate assemblages. Mater Struct 51(6):172
Standard Specifications for Concrete Structures—2007 (2010) Materials and construction
Stephant S, Chomat L, Nonat A, Charpentier T (2015) Influence of the slag content on the hydration of blended cement. Available from: https://cea.hal.science/cea-02509185
Taylor HFW (1998) Cement chemistry. T. Telford 459
Technical Guide (n.d.) Designing with precast concrete curing of high performance precast concrete. Available from: www.cpci.ca
Wang J, Long G, Xiang Y, Dong R, Tang Z, Xiao Q et al (2022) Influence of rapid curing methods on concrete microstructure and properties: a review. Case Stud Constr Mater 17:e01600
Wedatalla AMO, Jia Y, Ahmed AAM (2019) Curing effects on high-strength concrete properties. Adv Civil Eng 2019(1):1683292
Whittaker M, Zajac M, Ben Haha M, Bullerjahn F, Black L (2014) The role of the alumina content of slag, plus the presence of additional sulfate on the hydration and microstructure of Portland cement-slag blends. Cem Concr Res 66:91–101
Winter N (2009) Understanding cement. WHD Microanalysis Consultants Ltd., Suffolk
Winter N (2012) Scanning electron microscopy of cement and concrete. WHD Microanalysis Consultants Ltd., Farnham
Xu D, Tang J, Hu X, Yu C, Han F, Sun S et al (2023) The influence of curing regimes on hydration, microstructure and compressive strength of ultra-high performance concrete: a review. J Build Eng 76:107401
Zulu BA, Miyazawa S, Nito N (2019) Properties of blast-furnace slag cement concrete subjected to accelerated curing. Infrastructures. https://doi.org/10.3390/infrastructures4040069

Publisher's Note